



# Development and scaling of turbulent, twin round jets

Taye Melaku Tadesse<sup>1</sup> and Joseph Mathew<sup>1,†</sup>

<sup>1</sup>Department of Aerospace Engineering, Indian Institute of Science, Bangalore 560012, India

(Received 26 April 2021; revised 16 December 2021; accepted 27 February 2022)

The velocity field of stationary, turbulent, twin round jets has been found to scale with an intrinsic velocity  $U_0$  and length  $L_0$ , both depending linearly on inflow plane parameters – jet velocity  $U_j$ , diameter  $d$  and distance between jets  $S$ . Flow fields were obtained from large-eddy simulations at these conditions in two experiments: (1) at Reynolds number  $Re = 230\,000$  based on  $U_j$  and  $d$ , and  $S/d = 5$ ; and (2) at  $Re = 25\,000$ ,  $S/d = 2, 4, 8$ . Each jet develops independently and then merges into a single jet with an elliptic cross-section. Downstream, the jet becomes circular after a mild overshoot. Close quantitative agreement with experiment was obtained in all cases. As the merged jets develop, fluctuation levels over a central half-width are nearly uniform and scale with the local maximum mean velocity. In all cases, the mean streamwise velocity along the centreline of the configuration,  $U_c$ , rises to a peak  $U_0$  at a distance  $L_0$  from the inflow plane. The velocity  $U_0$  decreases and  $L_0$  increases with  $S$ . For all nozzle spacings, a similar development was observed:  $U_c/U_0$  is a function of distance  $x/L_0$  only, and is essentially independent of  $S/d$  and  $Re$ . Further, these intrinsic and input quantities are connected by simple relations:  $U_0 = U_j/(1.02S/d + 0.44)$  and  $L_0/d = 5.58S/d - 1.16$ . The far field development of the merged jet can also be scaled with  $U_0$  and  $S$ , analogous to round jet scaling with  $U_j$  and  $d$ . Thus all twin round jets may be described by these new intrinsic scales.

**Key words:** shear layer turbulence, turbulence simulation, jets

## 1. Introduction

Several canonical turbulent flows have been explored in great detail to understand fundamental features such as turbulent transport, scaling and flow development. These are plane and axisymmetric mixing layers, jets, wakes, channel and pipe flows, and boundary layers. All are models of flows encountered in nature and in engineering devices, sometimes with significant simplifications. In applications, these types of flows also

† Email address for correspondence: [joseph@iisc.ac.in](mailto:joseph@iisc.ac.in)

interact with others. An example is the use of multiple round jets rather than a single larger jet to provide the required mass flow rate. To obtain larger thrust, it is commonplace to find at least twin jets in aircraft, and a cluster of several jets in launch vehicles. Combustion chambers of gas turbines have an annular ring of many fuel injectors. Accounting for interactions among a jet pair, or multiple jets, is a crucial part of the design. It is thus useful to consider a twin jet configuration as a model that extends the library of canonical flows to understand interference effects.

Surprisingly little is available in the literature on twin jets, perhaps because such studies have been restricted to the specific configurations and needs of applications such as supersonic military aircraft. Although studies of plane, twin jets were available in Miller & Comings (1960), those for round, twin jets came much later. Measurements were reported by Okamoto *et al.* (1985) of a pair of round jets that emerged from a plane wall, termed unventilated jets, at a Reynolds number of 230 000, based on the jet exit velocity  $U_j = 47 \text{ m s}^{-1}$  and nozzle diameter  $d = 70 \text{ mm}$ . The distance between nozzle centres  $S/d$  was 5 and 8.06 in the two configurations reported. Mean velocity and pressure profiles were prepared from pressure probe data at several streamwise locations. For  $S/d = 5$ , individual jets developed like single jets for approximately  $17.5d$ , and then differences appeared as they merged downstream – by approximately  $25d$  – forming an elliptical cross-section that relaxed to a circular one downstream by approximately  $115d$ . For the larger nozzle spacing, merger occurs slightly farther downstream. After presenting these measurements, the paper turned to comparisons with an offset wall jet; i.e. as if the symmetry plane between the two jets were replaced by a plane wall. In the near field, these two flows are similar for approximately  $20d$  when  $S/d = 5$ . Of course, significant differences are to be expected downstream because twin jets relax into a combined round jet, whereas the latter develops as a wall jet. Harima, Fujita & Osaka (2001) and Harima, Fujita & Osaka (2005) reported mean and turbulence data, respectively, from their hot-wire measurements on unventilated twin round jets with nozzle spacings  $S/d = 2, 4$  and  $8$ , at  $Re = 25\,000$ . Yin, Zhang & Lin (2007) has provided velocity measurements for closely spaced nozzles with submerged water jets ( $S/d = 1.5, 1.75, 1.89; 3.3 \times 10^4 < Re < 8.33 \times 10^4$ ). Particle image velocimetry data for water jets with  $S/d = 1.5, 2.0, 3.0$  at  $Re = 3300$  are also available (Zang & New 2015). The most recent measurements were reported in Laban *et al.* (2019). The round jets were at  $Re = 10\,000$  and  $S/d = 2.8, 4.1, 5.5, 7.1$ . Profiles of streamwise velocity collapse on scaling with velocity half-width and centreline velocity of the individual jets before merger, and of the combined jet afterwards. Streamwise development in the individual jets scaled with local jet centreline velocity for all the internozzle spacings. The collapse is not as definite for Reynolds shear stress profiles, and not found for normal stress at all, but development along the centreline has little scatter for the different nozzle spacings. From velocity measurements along the configuration centreline, they tabulated the distance from the wall where the velocity reached a maximum. These quantities have a similar dependence on input parameters as in our solutions as discussed in § 4. Aleyasin & Tachie (2019) examined Reynolds number effects with experiments at  $Re = 5000, 10\,000, 14\,000$  and  $20\,000$  and  $S/d = 2.8$ , and concluded that velocity decay and jet spreading rates become independent of  $Re$  for  $Re > 10\,000$ . There are also two very specific computational studies of closely spaced, twin supersonic jets that seek to address aeroacoustics at take-off from aircraft carriers (Junhui, Xin & Xiaodong 2016; Goparaju & Gaitonde 2018).

The subject of this study is the structure of low speed, turbulent, twin round jets. A specific aim was to discover whether any universal scaling of twin round jets exists, since it has not been reported in any previous studies. The configuration comprises two

identical jets that emerge from the circular nozzle, bend towards each other, and merge to form a single jet. This is termed unventilated if the nozzle exits are flush with a common wall, and ventilated if there is no such wall – fluid from upstream of the nozzle exit will be drawn towards the emerging jets. One flow field was obtained from a large-eddy simulation (LES) at the conditions of the experiment reported in Okamoto *et al.* (1985) at a Reynolds number  $Re = 230\,000$  for  $S/d = 5$ . Three more LES were at  $Re = 25\,000$  for  $S/d = 2, 4$  and 8, which are the parameters for the experiments in Harima *et al.* (2001).

Profiles of velocity at several downstream stations, the development of velocity along the centreline of individual jets before merger, and thereafter along the centreline of the configuration, have been compared with experiment. Individual jets develop rather like single round jets initially and then become asymmetrical near merger. Some distance beyond merger, the combined jet relaxes to a single round jet, though the initial elliptical form exhibits axis switching. Along the configuration centreline the mean streamwise velocity  $U_c$  rises sharply at first and then decays. The peak of this rise,  $U_0$ , decreases with increasing  $S/d$  and its distance from the inflow plane,  $L_0$ , moves downstream. We find these two parameters,  $U_0$  and  $L_0$ , to be intrinsic scales on which the variation of centreline velocity collapses for all  $S/d$ . Further,  $L_0/d$  and the reciprocal  $U_j/U_0$  increase linearly with  $S/d$  – a simple relation between intrinsic scales and input parameters. Profiles over the cross-section show some dependence on the maximum mean velocity  $U_m$  at the section, even though it is still a developing flow – fluctuation amplitude collapses over a central region where the highest levels occur. Downstream of merger, like in single jets, profiles of mean velocity and Reynolds stresses collapse when scaled with local centreline velocity and local jet half-width. Thus we have a new, complete description of low-speed, turbulent, twin round jets. The initial development, including distance to merger, can be estimated from the dependence of the intrinsic scales ( $U_0, L_0$ ) on input parameters ( $U_j, d, S$ ), while the downstream development becomes that of single jets. Of course, other quantities that may be of interest to a designer, such as the development of mass flow rate (entrainment), may also be documented best by scaling with  $U_0$  and  $L_0$ . The numerical method and simulations are described in § 2, including the single round jet case that serves as a relevant validation and guide to setting up of twin jet simulations. Basic features of twin round jets are discussed in § 3 from the simulation of the experiment of Okamoto *et al.* (1985), followed by nozzle spacing effects in § 4.

## 2. Numerical method and simulations

All solutions were obtained by solving the Navier–Stokes equations for compressible flow (see, e.g. chapter 5, Tannehill, Anderson & Pletcher (1997)). The numerical method was implemented in an in-house code developed by, and as described in, Patel (2018). The code implements explicit, second-order, Runge–Kutta time stepping, and sixth-order compact differences for spatial derivatives on non-uniform grids. Here, a Cartesian grid was used, with non-uniform spacing for clustering at the shear layer near inflow, and stretching in geometric progression in lateral and streamwise directions. The LES is obtained by the explicit filtering method proposed in Mathew *et al.* (2003), which is a nearly equivalent implementation of the approximate deconvolution method (known as ADM) of Stolz & Adams (1999). Aside from the several flows reported when the approximate deconvolution method was developed, many more have been reported from Air Force Research Laboratory where the present filtering approach was used (e.g. Visbal & Rizzetta 2002; Rizzetta, Visbal & Morgan 2008). A similar approach, termed selective filtering has been used at École Centrale de Lyon for LES of jets (Bogey & Bailly 2006). Examples from our laboratory are in Patel (2018) and Mathew (2016).

Case	Flow	$Re$	$S/d$	$L_x/d$	$L_y/d$	$N_d$	$N_x$	$N_y$
SR120	Single jet	11 000	—	75	21	12	316	269
TR255	Twin jet	230 000	5	54	21	25	401	441
TR242	Twin jet	25 000	2	50	32	24	325	347
TR244	Twin jet	25 000	4	55	32	24	325	367
TR248	Twin jet	25 000	8	80	35	24	325	401

Table 1. Parameters of the LES. Case label indicates type of jet, number of points across jet diameter  $N_d$  and nozzle spacing. Here,  $L_z = L_y$  and  $N_z = N_y$ .

A Cartesian coordinate system is used with the  $x$ -axis aligned with the streamwise direction. Velocity components are  $u(x, y, z, t)$ ,  $v$ ,  $w$  in the  $x$ ,  $y$  and  $z$  directions. Means are  $U(x, y, z)$ ,  $V$ ,  $W$  and fluctuations are  $u'(x, y, z, t)$ ,  $v'$ ,  $w'$ . At the inflow plane, no-slip, isothermal conditions were specified at the wall. The jets were specified by setting the streamwise velocity component to have a top-hat profile with a tanh variation at the jet boundary. Cross-flow components were set to zero and pressure was set to a constant value. The density profile was then obtained from the Crocco–Busemann relation. Wherever the flow crosses a computational boundary, non-reflecting conditions, described in Poinso & Lele (1992) and termed NSCBCs, were applied. These boundary surfaces comprise the jet portion of the inflow plane, lateral boundary planes, and the downstream outflow plane. Near the lateral and outflow boundaries, there is a sponge layer where a smoothing filter was applied to transported variables (Bogey & Bailly 2002). The combination of the coarse mesh and filter causes fine scale fluctuations in the jet to disappear and ensures that there is no reverse flow at the outflow boundary. Then, standard, non-reflecting conditions are effective. The profiles at the inflow plane mentioned above are steady target values. Navier–Stokes characteristic boundary conditions applied at the inflow plane provides unsteady perturbations consistent with allowing waves from within to leave without reflection. A weighted sum of these unsteady profiles and the steady target profiles are applied as the boundary conditions on the inflow plane to prevent drift, as proposed in Bogey & Bailly (2006). It has not been necessary to add any fluctuations to the target profiles because these waves were sufficient to excite the shear layer instability.

The code has been validated extensively with tests ranging from acoustic wave propagation to LES of turbulent subsonic and supersonic (over- and under-expanded) jets (Patel 2018; Patel & Mathew 2019). Here, a simulation of a single round jet serves as a further validation relevant to the twin jet study. Grid requirements were understood from extensive single jet simulations.

Rectangular domains and Cartesian grids were used. Parameters of the different simulations are listed in table 1. Case SR120 is a single jet at  $Re = 11\,000$ , which is the well known benchmark experiment of Panchapakesan & Lumley (1993). In the cross-plane the grid was uniformly spaced over the cross-section of the jet up to  $1.5d$ , with spacing  $d/12$ , then stretched at 1% up to  $12.5d$ , and then at 10% until  $y = \pm L_y$  or  $z = \pm L_z$ . In table 1,  $N_d$  is the number of grid points across the diameter of the jet at the inflow plane. Grid spacing in the streamwise direction was increased from inflow itself at a uniform rate of 0.7%. There were 20 additional grid planes at the lateral boundaries and 31 at the outflow for sponge zones. Case TR255 is the experiment of Okamoto *et al.* (1985) with spacing  $S/d = 5$  at  $Re = 230\,000$ . In the  $y$ - $z$  plane, there are 25 gridpoints across each jet at inflow, uniform spacing up to  $4.5d$ , 1% stretching until  $10d$  and 10% beyond to the lateral boundaries. Streamwise stretch rate was 0.6%. Results of varying nozzle

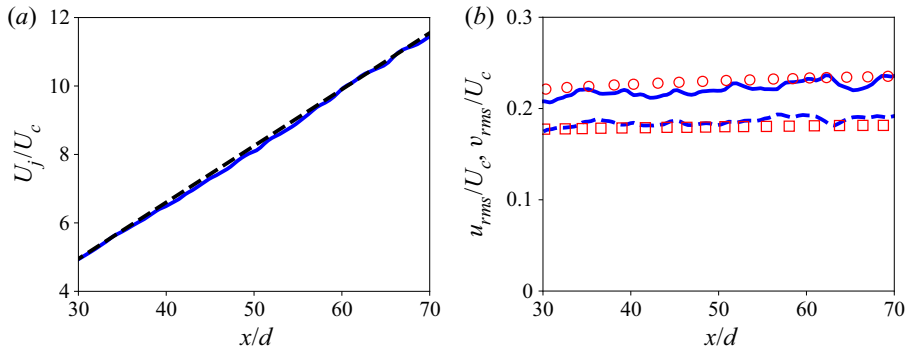


Figure 1. Self-preservation in mean and fluctuations of velocity in a single round jet at  $Re = 11\,000$  compared with the experiment of Panchapakesan & Lumley (1993). (a) Reciprocal of centreline velocity: LES (—, blue); experiment (---, black). (b) Velocity fluctuations: LES,  $u_{rms}$  (—, blue); LES,  $v_{rms}$  (---, blue); experiment,  $u_{rms}$  (○, red); experiment,  $v_{rms}$  (□, red).

spacing were obtained at the lower  $Re = 25\,000$  of the experiments in Harima *et al.* (2005). For these three cases the differences are the extent of the uniform region around the individual jet, and the larger cross-section of  $64d \times 64d$  ( $70d \times 70d$  for TR248). Typically, each simulation was run from the beginning for 10 nominal flow-through times so that a stationary state was obtained before collecting statistics from time series over 35 or more flow-throughs. Here, a flow-through time is the scale  $L_x/U_j$ , though fluid particles will take longer as the flow decelerates.

The single round jet at  $Re = 11\,000$  develops shear layer instabilities and subsequently breaks down into turbulence by  $x/d = 5$ . In the turbulent region, jet half-width grows linearly with growth rate 0.094, which is close to the value of 0.096 in Panchapakesan & Lumley (1993). The reciprocal of the mean centreline velocity  $U_c$ , scaled with its value  $U_j$  at the inflow plane, grows linearly with distance as shown in figure 1(a). The slope is  $1/6.06$ ; in the experiment too it was  $1/6.06$ . In under-resolved LES, the  $1/U_c$  curve will be slightly curved. Root mean square (r.m.s.) of fluctuations become very nearly constant when scaled with centreline velocity as shown in figure 1(b), as in the experiment.

Figure 2 shows radial profiles at several stations  $8 \leq x/d \leq 70$  of the mean and fluctuations of the streamwise velocity component. Profiles of the mean are still developing at  $8d$  and  $10d$ , but beyond  $15d$  there is no change when scaled with local centreline velocity  $U_c$  and half-width  $r_{1/2}$  (figure 2a). Close quantitative agreement with the profile from the experiments of Panchapakesan & Lumley (1993) has been obtained. Fluctuations also relax to a common profile on these scales. In figure 2(b) the two dashed curves are for  $x/d = 8, 15$ . Fluctuation levels in the LES are slightly smaller than in the experiment. Smoother curves and smaller variance would need longer sampling times, but it should be clear that scaled fluctuations also collapse. Profiles of the fluctuations of transverse component  $v_{rms}$  were similar (not shown here). Figure 3(a) shows power spectral density curves from time series of the streamwise velocity component along the jet axis at  $x/d = 35$  and  $48$ . A power-law region is evident and the spectra also collapse on local scales. These LES results are qualitative and quantitative indications of the adequacy of the simulations.

### 3. Structure of turbulent, twin round jets

Large-eddy simulations at the conditions of the experiment in Okamoto *et al.* (1985) at  $Re = 230\,000$ , corresponding to mean velocity at centreline,  $U_j = 47\text{ m s}^{-1}$ ,

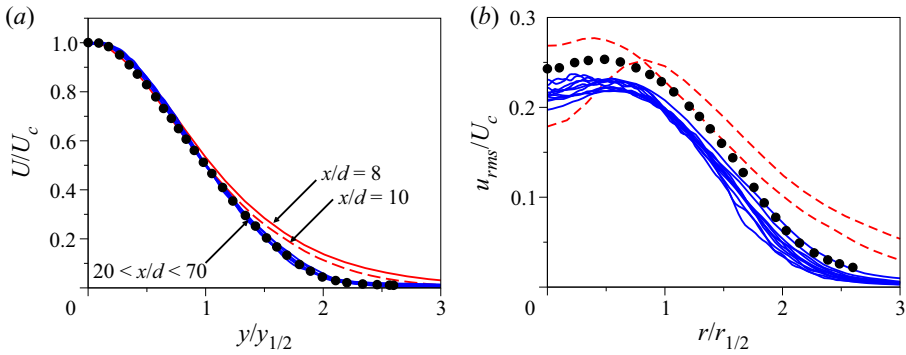


Figure 2. Radial profiles of mean and fluctuations of streamwise velocity component, scaled with local centreline velocity  $U_c$  and half-width  $r_{1/2}$ , from the single jet case SR120. (a) Profiles of streamwise component of mean velocity at  $x/d = 8, 10$  and  $15, 20, 25, \dots, 70$ . Profiles for  $15 \leq x/d \leq 70$  collapse to a single curve. Differences are seen for  $x/d = 8, 10$ . Symbols from the experiment of Panchapakesan & Lumley (1993), curves from LES. (b) Radial profiles of streamwise velocity fluctuations  $u_{rms}$  on planes  $x/d = 8, 10$  (---, red),  $15 \leq x/d \leq 65$  (—, blue); symbols from the experiment of Panchapakesan & Lumley (1993).

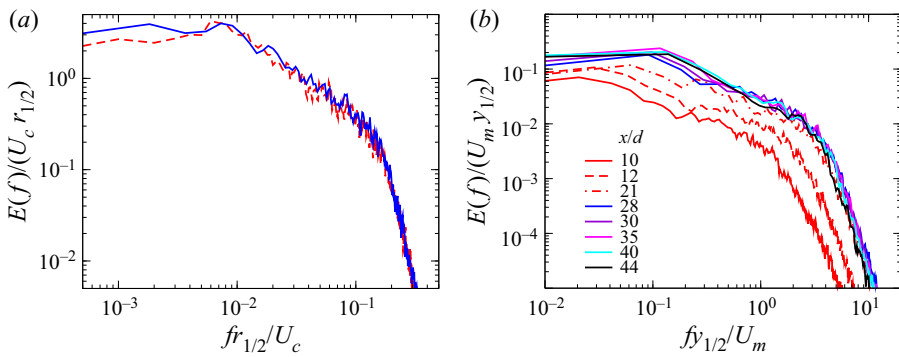


Figure 3. Power spectral density  $E(f)$  of streamwise velocity component  $u(x, 0, 0, t)$ . Scaled with local scales  $U_c$  and  $r_{1/2}$  (case SR120), and  $U_m$  and  $y_{1/2}$  (case TR255). (a) Single jet,  $x/d = 35$  (---, red),  $48$  (—, blue). (b) Twin jet.

were performed. Of the two configurations they reported, the following discussion is for  $S/d = 5$  (case TR255 in table 1). A test simulation was performed on a coarser grid which had 10 points across each jet at inflow, resulting in a grid of size  $203 \times 159 \times 159$  points. By comparing velocity profiles at several stations it was observed that, everywhere, the finer grid solution agreed more closely with experiment. This convergence with improving spatial resolution was expected because it has been observed to be a feature of the present LES model in many previous examples (Mathew *et al.* 2003; Mathew 2016). A significant difference (error) on the coarse grid was that the large scales were more active and the merger took place earlier, completed by  $35d$ , whereas in the experiment, and on the finer grid, merger is approximately  $10d$  farther downstream.

An impression of the twin jet solution can be obtained from the visualization in figure 4 where isosurfaces of velocity magnitude are shown. Laminar jets emerge from the nozzles and roll up into rings which break down into turbulence. These turbulent jets merge to form a single jet, initially with an elliptic cross-section.

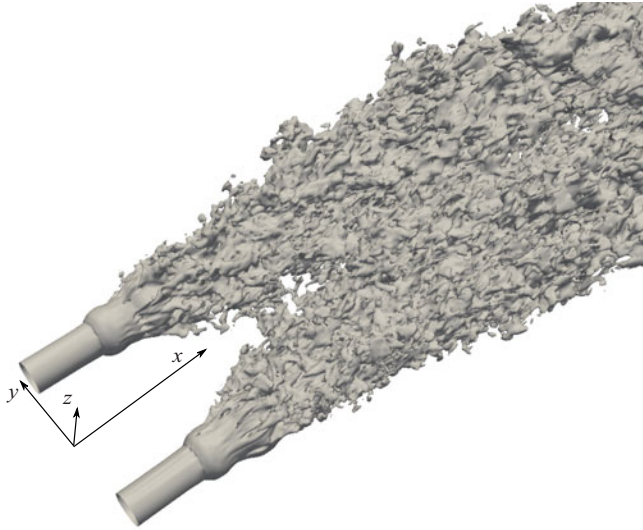


Figure 4. A twin round jet visualized with isosurfaces of velocity magnitude at an instant from case TR255.

### 3.1. Mean quantities

Figure 5 shows distributions of the streamwise velocity component at an instant, and the mean, together with a few streamlines. The boundary conditions permit weak flows to enter from the lateral boundaries and get entrained by the jets. Note that there is no significant bending of the jets towards each other – unlike in twin plane jets; so the initial development is rather like that of single jets. The development of jet velocity  $U_n$  on the lines  $y = \pm S/2$ ,  $z = 0$  through the nozzle centres, and  $U_c$  along the configuration centreline ( $y = z = 0$ ), are compared with experiment in figure 6(a). The maximum velocity  $U_m(x)$  at a section is the larger of  $U_n(x)$  and  $U_c(x)$ . Initially  $U_m(x)$  occurs on the nozzle axis; during merging, it moves to the  $x$ -axis. The velocity  $U_m(x)$  from simulation is compared with experiment in figure 6(b). Okamoto *et al.* (1985) had used  $U_m$  to normalize the velocity data. Here we find it to permit some, limited, scaling of the data. We will also use the distance  $y_{1/2}$  from the configuration axis to the point where the velocity  $U(x, y; z = 0)$  falls to  $U_m(x)/2$  as a local reference length, analogous to the half-width of single jets.

From time series  $u(x, 0, 0, t)$  at stations along the  $x$ -axis, the development of the energy spectrum normalized using  $U_m$  and  $y_{1/2}$  is shown in figure 3(b). Beyond  $x/d = 28$ , the spectra do collapse even though merger is not yet complete and  $U_m$  is not yet on the configuration centreline (see figure 8a below). It is perhaps not surprising then that fluctuation levels over a central part of the merged jet also scale with  $U_m$  (see figure 9 and discussion below).

Jet width growths are shown in figure 7, by taking jet boundary to be where  $U = 0.1U_m$ , as reported in the experiment, instead of the more common half-width. The merging jets occupy an elliptical region, with the major axis in the  $x$ - $y$  plane, which then relaxes to a circular region with a slight over-shoot. Growth of the half-width of single round jets has been included, but it is worth remembering that measurements near the outer edges of shear flows are not as reliable due to flow reversals. The initial spreading in the  $x$ - $y$  plane is slightly smaller than that of single jets in both LES and experiment – differences are smaller downstream of merger. Axis switching appears as a mild reversal in growth. In the  $x$ - $z$  plane of the nozzle axis of either jet ( $y = S/2$ ), growth rates in LES and experiment

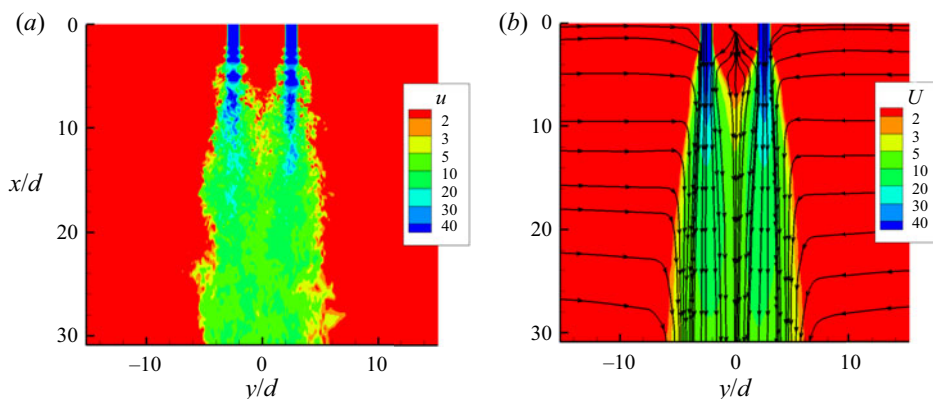


Figure 5. Streamwise component of velocity on plane  $z = 0$  from LES of case TR255. (a) Streamwise velocity  $u(x, y, 0, t)$  ( $\text{m s}^{-1}$ ). (b) Mean streamwise velocity  $U(x, y, 0)$  ( $\text{m s}^{-1}$ ) and streamlines.

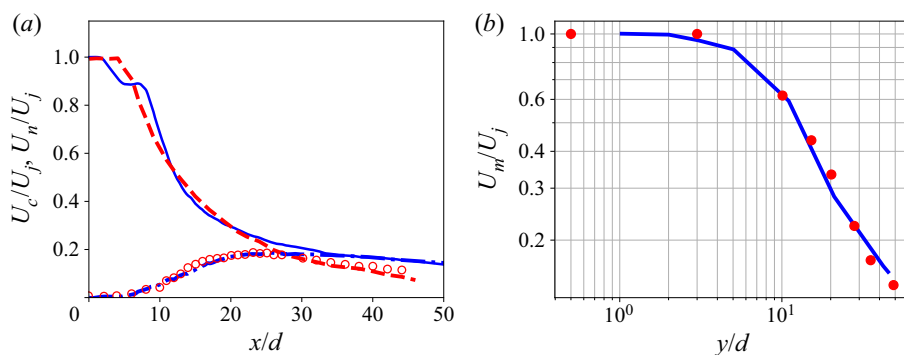


Figure 6. Development of mean streamwise velocity for case TR255. (a) Decay compared with measurement along nozzle axis:  $U_n$ , LES (—, blue);  $U_n$ , experiment (---, red);  $U_c$ , LES (●, blue);  $U_c$ , experiment (○, red). (b) Maximum at any cross-section, initially within individual jets and along  $x$ -axis after jets merge:  $U_n$ , LES (—, blue);  $U_c$ , experiment (●, red).

are closer to that of single jets. Due to possible differences in inflow conditions, evident in velocity  $U_n(x)$  also (figure 6a), the widths in figure 7(b) are different for  $x/d < 10$ , but the slopes are very nearly the same downstream. We shall return to this below while discussing pressure distributions.

Profiles of mean velocity at several downstream locations are shown in figure 8(a). Before merging, the maximum velocity is still within individual jets ( $x/d = 20, 28$ ), but the velocity in the region between the jets is increasing (is within 90 % of  $U_m$  at  $x = 35d$ ). Generally, there is very close quantitative agreement with experiment over most of the jet. Small differences are evident near the outer boundary for  $x > 28d$ .

Figure 8(b) is a comparison of radial pressure profiles between LES and experiment. Close quantitative agreement has been obtained. The pressure coefficient  $C_p = (p - p_\infty) / \frac{1}{2} \rho_\infty U_j^2$ , where  $p_\infty$  and  $\rho_\infty$  are the pressure and density in the far field. The pressure is generally considered to be uniform in free shear flows. But, there is a small gradient across the shear layer which would balance fluctuations of the radial component of velocity (Tennekes & Lumley 1972, chapter 4). The approximation is acceptable since the maximum difference in pressure is small: it is only approximately 0.1 % of the inflow



### Turbulent, twin round jets

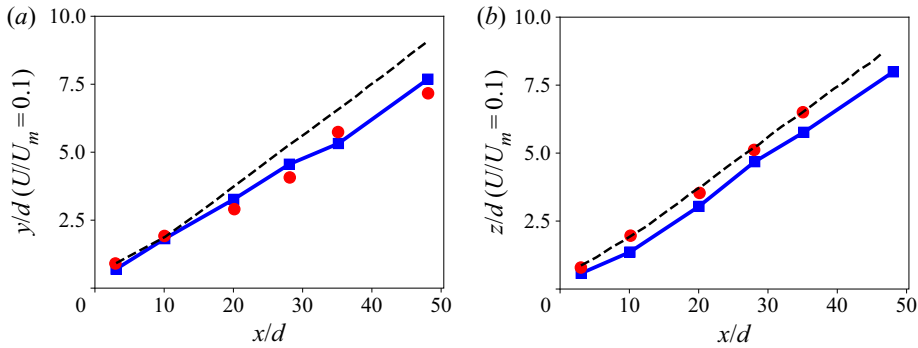


Figure 7. Jet spreading in two planes. Jet boundary is located where mean velocity  $U$  is 10% of the maximum over cross-section ( $x$ , constant): experiment ( $\bullet$ , red); LES ( $\blacksquare$ , blue); single jet ( $---$ ). (a) On  $z = 0$  and (b) on  $y = S/2$ .

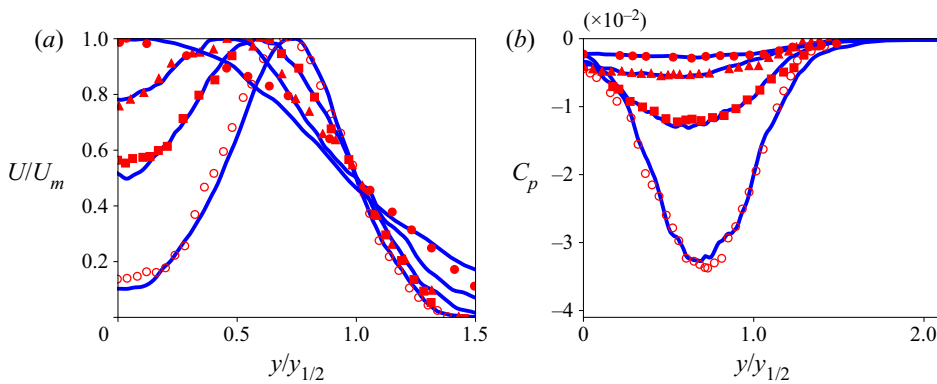


Figure 8. Radial profiles of mean streamwise velocity and pressure coefficient for case TR255: blue curves, LES; symbols (experiment, Okamoto *et al.* 1985) at  $x/d = 10$  ( $\circ$ , red), 20 ( $\blacksquare$ , red), 28 ( $\blacktriangle$ , red), 48 ( $\bullet$ , red). (a) Streamwise velocity. (b) Pressure coefficient.

plane dynamic pressure in the single jet region (see curve for  $x/d = 48$  in figure 8b). In the twin jet configuration, we observe the pressure difference to be significantly larger before the jets merge – approximately 3%–4% of dynamic pressure at  $x/d = 10$ . In turn, this radial gradient would be consistent with a slightly smaller radial spreading than in a uniform pressure field. In figure 7(a), the spreading of the twin jet in the  $x$ - $y$  plane is slightly less than that of single jets initially but appears to be at nearly the same rate beyond  $x/d = 40$ . As the merged elliptic form relaxes to a round jet, and the radial pressure gradient diminishes, the difference in spread rate should also disappear. The difference between twin jet and single jet is noticeably less in the  $x$ - $z$  plane; consistently, the maximum difference in  $C_p$  across the jet in  $x$ - $z$  planes was found to remain less than  $-0.003\%$  of dynamic pressure (not shown).

### 3.2. Turbulence intensities and Reynolds shear stress

Okamoto *et al.* (1985) had not provided turbulent fluctuation measurements. In single jets, turbulence intensity scales with the mean centreline velocity, and radial extent on the half-width. In twin jets, we may expect the same scaling to hold good far downstream.

In the developing region, by definition, we do not expect any such scaling. However, it turns out that fluctuations do scale with the maximum velocity  $U_m$  even where the merged jet is developing into the round jet. Figure 9 shows profiles of fluctuations along two lines ( $y; z = 0$ ) and ( $y = 0; z$ ) at several  $y$ - $z$  planes. Quantities are normalized with  $U_m$  and length  $y_{1/2}$ .

Consider first figure 9(a,c,e,g). Curves with red symbols for  $x/d = 8, 10, 15$  show the development of fluctuations. The continuous ones are for  $20 \leq x/d \leq 50$ . Generally, for  $x/d > 20$ , all the curves collapse over  $y < y_{1/2}$  which is the width of a core region wherein fluctuation levels are nearly uniform and scale with  $U_m$ . In single round jets also, fluctuation levels are nearly uniform within the half-radius (Panchapakesan & Lumley (1993); figure 2b). The length  $y_{1/2}$  is a scale for jet width before merger ( $x/d < 20$ ) and thereafter for the extent of the turbulent core, but not the jet width. Of course, since the fluctuation levels in the core are nearly uniform, these curves suggest a common profile on a shifted local coordinate  $(y - y_{1/2})/\delta$ , where  $\delta$  would be the width over which the velocity  $U(y)$  drops from  $U_m$  to zero. Figure 9(b,d,f,h) contains profiles along the  $z$ -axis. Since the turbulence level is larger near the centre of the individual jets even as they merge, fluctuations levels in the  $y = 0$  plane continue to develop for quite some distance downstream. In figure 9(b),  $u_{rms}/U_m$  approaches its downstream value by  $x/d \approx 30$  near the axis but the extent of this region continues to increase. The development of transverse fluctuation to the far downstream levels (amplitude and extent of region) is not very different. Figure 9(g) shows the development of Reynolds shear stress component  $\langle u'v' \rangle$  along  $y, z = 0$ . The distribution for  $x/d \leq 40$  is consistent with an outer and inner shear layer of the individual jets. It is only by  $x/d = 45$  that traces of the inner shear layer has ended. Figure 9(h) shows the development of component  $\langle u'w' \rangle$  along  $z, y = 0$ ; these profiles have the same shape but other scales for velocity and extent are needed.

All the comparisons with the experiment of Okamoto *et al.* (1985) serve to confirm that the LES provides a very accurate description of large scale features of twin round jets at the large Reynolds number, 230 000, of relevance to practical applications. Okamoto *et al.* (1985) had used the maximum velocity  $U_m$  at streamwise stations to normalize the data. We observe from the simulation data that  $U_m$  is a velocity scale for turbulent fluctuations. In the following section, we examine the effects of nozzle spacing  $S$ .

#### 4. Nozzle spacing effects

Nozzle spacing effects were studied by performing LES at the conditions in Harima *et al.* (2005) for three nozzle spacings  $S/d = 2, 4$  and  $8$  at  $Re = 25\,000$ . Turbulence scalings are well-established in round jets by  $Re \sim O(10^4)$  itself; e.g. the benchmark by Panchapakesan & Lumley (1993) is at 11 000. Simulation domain and grid sizes are listed in table 1. Grids are similar in all cases, with 24 points across the jet, uniform spacing to  $1.5d$  around each jet and then mild stretching outward ending with a coarsely spaced buffer zone.

The solutions are shown in figure 10 as contours of the streamwise velocity at an instant on the plane  $z = 0$ . Not surprisingly, flow fields of all cases are similar to the solution for  $S/d = 5$  that was discussed in § 3 above. Each jet grows by turbulent entrainment with little effect on the other until both become part of an initially elliptical region. Merging occurs farther downstream as  $S/d$  is increased. Mean fields revealed that there is a mild bending towards each other when the spacing is large ( $S/d = 8$ ); the bending is quite small even at  $S/d = 5$  (see figure 5b above). When the nozzle spacing is quite small, the jets begin to interact before breakdown to turbulence is completed: figure 10(a) for  $S/d = 2$  shows merger to begin at the vortex ring stage itself; when the spacing is larger, say,  $S/d = 4$  (figure 10b), individual jets have broken down before merger begins.

Turbulent, twin round jets

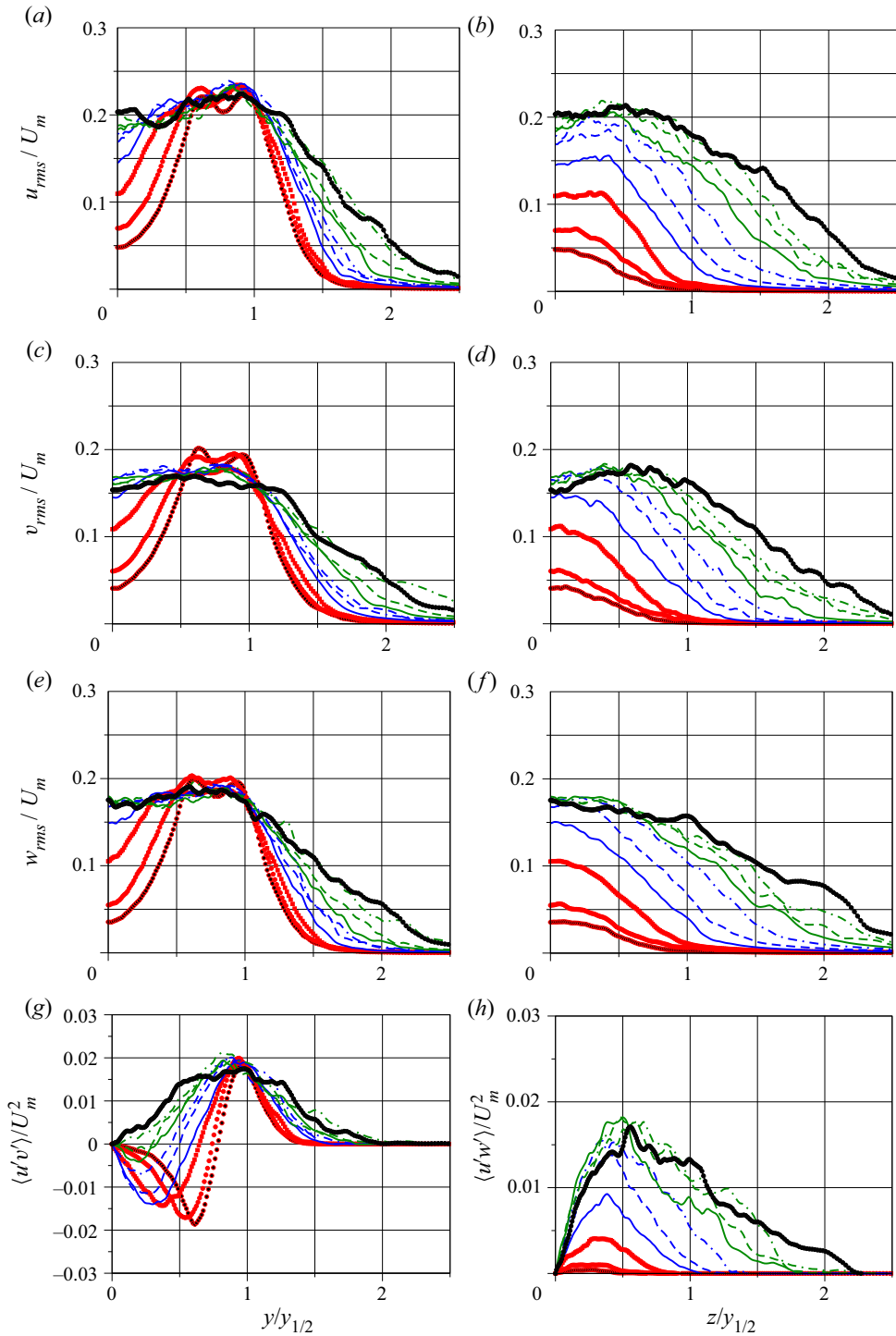


Figure 9. (a–f) Fluctuation profiles and (g,h) Reynolds shear stress profiles. All are normalized with maximum of local mean streamwise velocity  $U_m$  and distance  $y_{1/2}$ . Here,  $x/d = 8$  (○, red), 10 (●, red), 15 (■, red), 20 (—, blue), 25 (---, blue), 30 (-●-, blue), 35 (—, green), 40 (---, green), 45 (-●-, green), 50 (-○-).

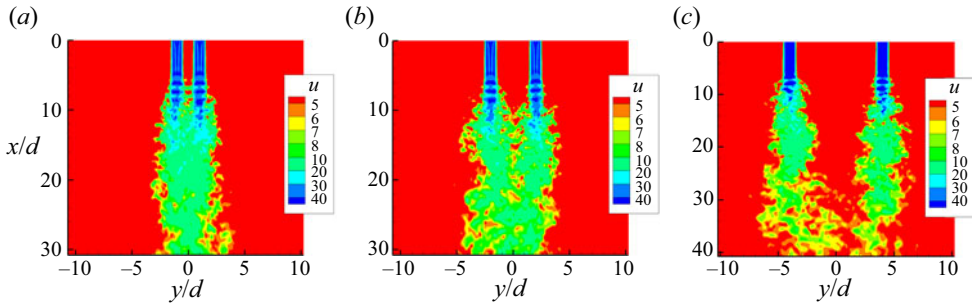


Figure 10. Streamwise component of velocity at an instant on plane  $z = 0$  from LES at  $Re = 25\,000$ . (a)  $S/d = 2$ , (b)  $S/d = 4$ , (c)  $S/d = 8$ .

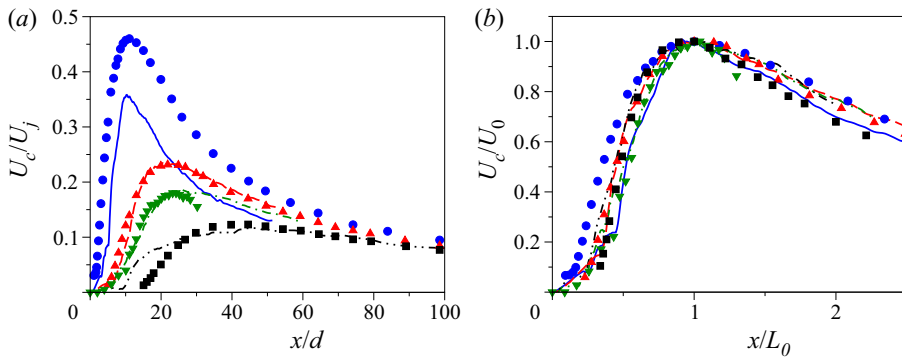


Figure 11. Development of streamwise velocity along configuration axis  $y = 0, z = 0$  for  $2 \leq S/d \leq 8$ . (a) Scaled with input parameters;  $U_c(x)$ . (b) Scaled with peak velocity  $U_0$  and distance to peak  $L_0$ ;  $U_c(x)$  scaled with  $U_0$  and  $L_0$ . For LES:  $S/d = 2$  (—, blue), 4 (---, red), 5 (-•-, green), 8 (-••-,). For experiment (Harima *et al.* 2001):  $S/d = 2$  (•, blue), 4 (▲, red), 8 (■). For experiment (Okamoto *et al.* 1985):  $S/d = 5$  (▼, green).

Thus, the initial development for  $S/d = 2$  is different from the others. Large spacing brings in differences to later development: for  $S/d = 8$ , there is a mild bending of the two jets towards each other, and the larger aspect ratio of the elliptic region on merger results in a slower relaxation to a single round jet.

For turbulent single round jets that emerge from a nozzle of diameter  $d$  with a near uniform velocity  $U_j$ , these input parameters serve as scales for the configuration. Local, intrinsic scales are the centreline velocity  $U_c$  and half-width  $r_{1/2}$ . Assuming self-preservation, we can derive power law relations for these local scales in terms of the input parameters  $U_j$  and  $d$ . Experiments show these relations to hold from a short distance downstream of the breakdown to turbulence. For twin round jets, the input parameters are  $U_j, d$  and  $S$ . It is reasonable to expect the far downstream structure to be similar to single jets. However, we find that the near field also has intrinsic scales on which the development collapses into a single curve for the range of nozzle spacings simulated.

Curves in figure 11(a) are of the development of mean streamwise velocity along the configuration centreline  $U(x, y = 0, z = 0)$  from the four twin-jet simulations and the two experiments. There is an initial rise as jets interact and then a decay in the combined jet. The growth and decay are sharper for closely spaced nozzles; the peak value is smaller and occurs increasingly farther downstream as nozzle spacing increases because centreline velocities of individual jets will have decayed more before merging. The data from the

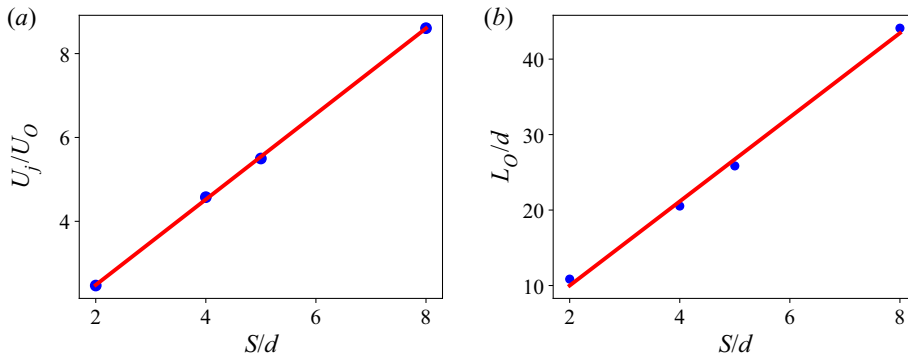


Figure 12. Dependence of intrinsic scales on nozzle spacing. (a) Maximum of centreline velocity,  $U_0$ . (b) Distance  $L_0$  from inflow plane. Here, LES (●, blue); linear fit (—, red).

simulations are very close to those from the experiments for  $S/d = 4$  (Harima *et al.* 2001) and  $S/d = 5$  (Okamoto *et al.* 1985), but clearly different for the other two cases. We suppose the differences to be due to differences in conditions at the nozzle exit. In turn there are effects on the initial development: as pointed out while discussing figure 10, the closely spaced jets merge before breakdown to turbulence is completed, while at the largest spacing there is a slight bending towards each other. So, no attempt was made to find an inflow condition that would give closer agreement with Harima *et al.* (2001) for all spacings. In spite of such differences, it turns out that data from both experiment and simulation support a new intrinsic scaling.

Let  $U_0$ , the maximum of  $U_c$ , be a velocity scale, and the distance from the wall  $L_0$  where this maximum is reached be a length scale. Remarkably, when the development of centreline velocity is rescaled,  $U_c/U_0$  is seen to be a function of  $x/L_0$ , independent of  $S/d$  (figure 11b). So, these are intrinsic length scales of the similar, initial development of twin jets. It remains to connect these intrinsic scales to the input parameters. Figure 12(a) shows the dependence of  $U_0$  scaled with jet inflow velocity  $U_j$  on  $S/d$ . Over this range, for the LES data,  $U_0/U_j = 1/(1.02S/d + 0.44)$ . The length scale also has an essentially linear dependence:  $L_0/d = 5.58S/d - 1.16$  (figure 12b). For the experiments of Harima *et al.* (2001),  $U_0/U_j = 1/(0.98S/d + 0.27)$  and  $L_0/d = 5.6S/d - 0.31$ . Laban *et al.* (2019) had performed experiments on twin round jets with  $S/d = 2.8, 4.1, 5.5$  and  $7.1$  at  $Re = 10\,000$ . They have provided the maximum mean velocity on the centreline and the distance to the location ( $U_0$  and  $L_0$  in our notation). A linear fit to their data gives  $U_0/U_j = 1/(1.04S/d + 1.13)$  and  $L_0/d = 5.51S/d + 0.71$ . Thus there is close quantitative agreement on the slopes for the dependence of both scales on the spacing in all three studies. The differences in the intercepts could be due to differences in inflow profiles, and perhaps a Reynolds number effect, similar to differences in the virtual origin in the linear relation for centreline velocity decay in a single round jet. Though all three experiments were of unventilated jets, Okamoto *et al.* (1985) have used nozzles with a smooth contraction, Harima *et al.* (2001) had a uniform pipe of length  $2d$ , and Laban *et al.* (2019) had conical nozzles and had noted the *vena contracta* formation.

The development of fluctuations  $u_{rms}$  along the configuration axis is compared with the data from the experiments of Harima *et al.* (2005) in figure 13. Very close quantitative agreement has been obtained at all three nozzle spacings. When rescaled with  $U_0$  and  $L_0$ , all curves collapse, providing further support for this scaling (figure 13b). Although the rescaling brings these curves much closer together, small differences can be discerned.

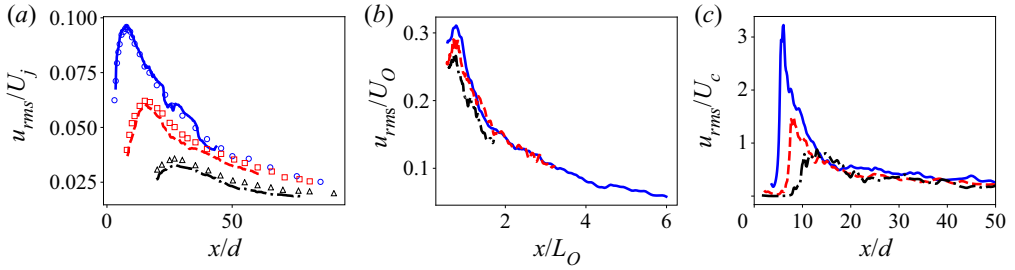


Figure 13. Development of streamwise velocity fluctuations along configuration axis  $y = 0, z = 0$  from LES (a) scaled with  $U_j$  and  $d$ , (b) scaled with  $U_0$  and  $L_0$ , (c) scaled with  $U_c$ . Here,  $S/d = 2$  (—, blue), 4 (---, red), 8 (-●-●-). Data from experiments (Harima *et al.* 2005) in (a) with  $S/d = 2$  (○, blue), 4 (●, red), 8 (■).

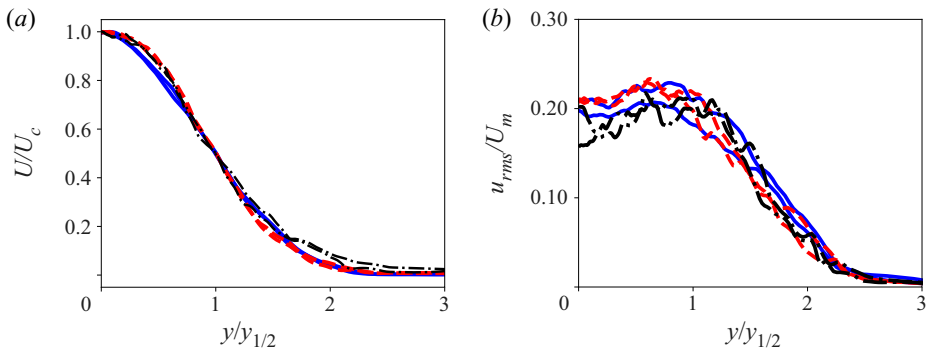


Figure 14. Spanwise profiles of (a) mean streamwise velocity ( $U/U_c$ ) and (b) fluctuations ( $u_{rms}/U_m$ ). Here,  $S/d = 2, x/d = 30, 40$  (—, blue);  $S/d = 4, x/d = 45, 50$  (---, red);  $S/d = 8, x/d = 70, 80$  (-●-●-).

Over the very short range upstream of the peak the differences are larger; downstream of the peak the curves for  $S/d = 2$  and 4 are more nearly coincident, whereas that for  $S/d = 8$  is not. We suppose these differences to arise from transition and the development of turbulence in the jets. In single round jets it is well known that fluctuations decay with downstream distance, but maintain a constant level when scaled with the local centreline velocity – also obtained in single jet LES discussed above (see, figure 1b). Figure 13(c) shows the development in twin jets. Beyond  $x/d \approx 20$ , all three jets exhibit nearly the same level of fluctuations when scaled with the configuration centreline velocity  $U_c$ . Thus, the flow upstream of merger collapses into one when scaled with  $U_0$  and  $L_0$ , while downstream, in the merged jet, the relevant scale is the centreline velocity  $U_c$ . This far-field scaling, exactly as in single jets, is supported by the collapse of radial profiles of the mean streamwise velocity and its fluctuations. Figure 14(a) shows mean streamwise velocity scaled with  $U_c$  and scaled with half-width  $y_{1/2}$  for the three simulations, at two stations each, downstream of merging. Clearly, on these scales the profiles are independent of  $S$ . Similarly, as figure 14(b) shows, fluctuation profiles also collapse.

Just as the local structure in the merged jet (spanwise profiles) is characterized by centreline velocity and half-width, the decay of these local scales is similar to that of single jets; i.e.  $U_c \sim 1/x$  and  $y_{1/2} \sim x$ . If it is the merged jets that are similar, it seems reasonable to ask whether they develop as if from a jet of an equivalent diameter. Noting that the initial development (upstream of merger) scales with  $U_0$  and  $L_0$ , we may suppose these two to be the relevant scales for the merged jet. Furthermore, since  $L_0$  depends linearly on  $S$

## Turbulent, twin round jets

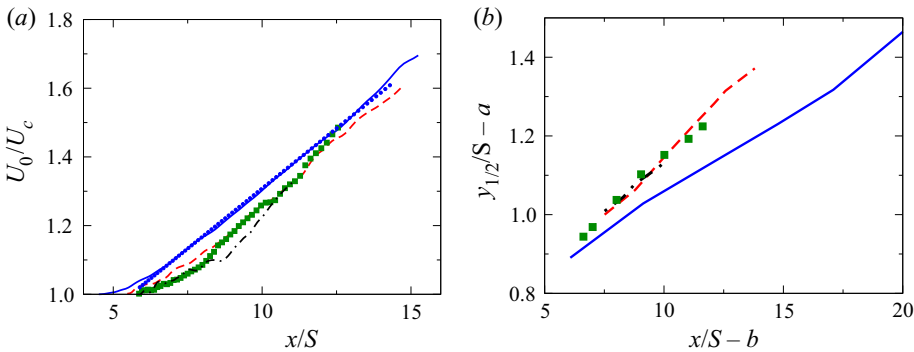


Figure 15. Development of (a) mean centreline velocity and (b) half-width. Here,  $S/d = 2$  (—, blue), 4 (---, red), 5 (■, green), 8 (●-●-). Linear fit to the velocity development for  $S/d = 2$  in panel (a) above is shown as a dotted line. Curves in panel (b) have been translated to show the nearly similar development for  $S/d = 4, 5, 8$ .

(figure 12b), we may suppose the merged jet to develop as if from velocity  $U_0$  and size  $S$ , analogous to inflow velocity  $U_j$  and diameter  $d$  of single jets. Figure 15(a) shows the streamwise development of centreline velocity for all four twin round jets. On  $U_0$  and  $S$ , the reciprocal of the centreline velocity increases linearly with distance in approximately the same way, independent of  $S$ . An approximate relation is  $U_0/U_c = 0.0713(x/S)$ , from the linear fit of the curve for  $S/d = 2$ . A linear development may be taken as a leading-order approximation only. Nonlinear development and differences arising from nozzle spacing are also evident. For the small spacing of  $S/d = 2$ , the nonlinear initial portion does not persist beyond  $x/S \approx 7$ . Several slope changes are evident for  $S/d = 5$ .

Half-widths also grow linearly, at the same rate in all four jets when scaled with  $S$ , almost independently of  $S$ . In figure 15(b) jet half-widths have been plotted against streamwise distance, scaled with  $S$ . Curves have been translated by different amounts  $a$  and  $b$  to see the agreement on slope. Except for  $S/d = 2$ , on translating these curves, it is clear that the spreading rate is nearly the same, independent of  $S$ . For the closest spacing, the initial spreading rate is noticeably smaller; a comparable slope is found only far downstream. Excluding the  $S/d = 2$ , the linear fit through all points for  $4 < S/d < 8$  in figure 15(b), has the slope 0.059. To leading order, the downstream development of the merged jet may be viewed as that of an equivalent round jet with an initial velocity of  $U_0$  and diameter  $S$ .

## 5. Conclusions

From an analysis of flow fields from LESs of pairs of identical turbulent round jets, emerging from ports in a plane wall, an intrinsic velocity scale  $U_0$  and length scale  $L_0$  were identified. Especially, the near-field solution between the wall and the merger was found to have a clear dependence on these scales. Simple, linear relations connect these scales to the configuration parameters at the inflow plane, namely, jet velocity  $U_j$ , jet diameter  $d$  and distance between ports  $S$ . In the far field, after the two jets merge and develop into a single round jet,  $U_0$  and  $S$  seem to be analogous to  $U_j$  and  $d$  of single, round turbulent jets. It is not necessarily universal across all twin round jets. Here, since the inflow conditions are the same (thin bounding shear layers enclosing a uniform velocity jet), the initial development of individual jets is the same in all cases. Differences due to fully developed laminar inflows, or turbulent inflows must be considered separately.

We can understand this scaling from the following argument. As each jet develops independently, their centreline velocities fall as  $1/x$ . The peak velocity along the configuration centreline can be expected to be of the order of individual jet centreline velocity near the merger point. Since the distance to this peak  $x = L_0$  should vary as  $S$ , and was found to be so (figure 12b), we may also expect  $U_0 \sim 1/S$ . We may expect a more complex dependence as the  $S$  becomes very large because at merger the jet will occupy an elliptic region with a large aspect ratio  $O(S/d)$ .

Merger is a relatively slow development becoming complete over many diameters – two jets are still evident in the velocity profiles at 28 diameters when the nozzle spacing was only five diameters (figure 8a). So it is fortunate that in the merging region the maximum velocity  $U_m$  across a downstream plane was found to be a useful local scale to estimate the peak levels of turbulence in the plane, and the extent of this region to be  $y_{1/2}$ .

This identification of intrinsic scales  $U_0$  and  $L_0$  in terms of  $U_j$ ,  $d$  and  $S$ , provides a simple method to design twin jet configurations. It is also an indication that such scaling may exist for an array of identical jets. Quantities of interest, such as the growth of mass fluxes (entrainment), can be documented in terms of the intrinsic scales, to serve as a starting point for design of engineering devices.

**Acknowledgements.** We thank Dr S.K. Patel for giving his compressible flow solver, and for helpful discussions on the computations. We thank SERC, IISc for use of the CRAY XC40.

**Declaration of interests.** The authors report no conflict of interest.

**Author ORCIDs.**

Joseph Mathew <https://orcid.org/0000-0002-4437-8262>.

#### REFERENCES

- ALEYASIN, S.S. & TACHIE, M.F. 2019 Statistical properties and structural analysis of three-dimensional twin round jets due to variation in Reynolds number. *Intl J. Heat Fluid Flow* **76**, 215–230.
- BOGEY, C. & BAILLY, C. 2002 Three-dimensional non-reflective boundary conditions for acoustic simulations: far field formulation and validation test cases. *Acta Acust. United Acust.* **88**, 463–471.
- BOGEY, C. & BAILLY, C. 2006 Computation of a high Reynolds number jet and its radiated noise using large eddy simulation based on explicit filtering. *Comput. Fluids* **35**, 1344–1358.
- GOPARAJU, K. & GAITONDE, D.V. 2018 Dynamics of closely spaced supersonic jets. *J. Propul. Power* **34** (2), 327–339.
- HARIMA, T., FUJITA, S. & OSAKA, H. 2001 Mixing and diffusion processes of twin circular free jets with various nozzle spacing. In *5th World Conference on Experimental Heat Transfer, Fluid Mechanics, and Thermodynamics* (ed. G.P. Celata), pp. 1017–1022.
- HARIMA, T., FUJITA, S. & OSAKA, H. 2005 Turbulent properties of twin circular free jets with various nozzle spacing. In *Engineering Turbulence Modelling and Experiments* (ed. W. Rodi), vol. 6, pp. 501–510. Elsevier.
- JUNHUI, G., XIN, X. & XIAODONG, L. 2016 Numerical simulation of supersonic twin-jet noise with high order finite difference scheme. *AIAA Paper* 2016-2938.
- LABAN, A., ALEYASIN, S.S., TACHIE, M.F. & KROUPRIYANOV, M. 2019 Experimental investigation of nozzle spacing effects on characteristics of round twin free jets. *J. Fluids Engng Trans. ASME* **141** (7), 1–11.
- MATHEW, J. 2016 Explicit filtering for large eddy simulation as use of a spectral buffer. [arXiv:1610.01738](https://arxiv.org/abs/1610.01738).
- MATHEW, J., LECHNER, R., FOYSI, H., SESTERHENN, J. & FRIEDRICH, R. 2003 An explicit filtering method for large eddy simulation of compressible flows. *Phys. Fluids* **15** (8), 2279–2289.
- MILLER, D.R. & COMINGS, E.W. 1960 Force-momentum fields in a dual-jet flow. *J. Fluid Mech.* **7**, 237–256.
- OKAMOTO, T., YAGITA, M., WATANABE, A. & KUWAMURA, K. 1985 Interaction of twin turbulent circular jet. *Bull. JSME* **28** (238), 617–622.
- PANCHAPAKESAN, N.R. & LUMLEY, J.L. 1993 Turbulence measurements in axisymmetric jets of air and helium. Part 1. Air jet. *J. Fluid Mech.* **246**, 197–223.



## *Turbulent, twin round jets*

- PATEL, S.K. 2018 Adaptive filtering for large eddy simulation of flows with shocks and its application to launch pad deflectors. PhD thesis, Department of Aerospace Engineering, Indian Institute of Science.
- PATEL, S.K. & MATHEW, J. 2019 Shock capturing in large eddy simulations by adaptive filtering. *Fluids* **4**, 132.
- POINSOT, T.J. & LELE, S.K. 1992 Boundary conditions for direct simulations of compressible viscous flows. *J. Comput. Phys.* **101**, 104–129.
- RIZZETTA, D.P., VISBAL, M.R. & MORGAN, P.E. 2008 A high-order compact finite-difference scheme for large-eddy simulation of active flow control. *Prog. Aerosp. Sci.* **44** (6), 397–426.
- STOLZ, S. & ADAMS, N.A. 1999 An approximate deconvolution procedure for large-eddy simulation. *Phys. Fluids* **11**, 1699.
- TANNEHILL, J.C., ANDERSON, D.A. & PLETCHER, R.H. 1997 *Computational Fluid Mechanics and Heat Transfer*, 2nd edn. Taylor & Francis.
- TENNEKES, H. & LUMLEY, J.L. 1972 *A First Course on Turbulence*, 1st edn. MIT Press.
- VISBAL, M.R. & RIZZETTA, D.P. 2002 Large-eddy simulation on curvilinear grids using compact differencing and filtering schemes. *J. Fluids Engng* **124**, 836–847.
- YIN, Z.-Q., ZHANG, H.-J. & LIN, J.-Z. 2007 Experimental study on the flow field characteristic in the mixing region of twin jets. *J. Hydrodyn.* **19** (3), 309–313.
- ZANG, B. & NEW, T.H. 2015 On the wake-like vortical arrangement and behaviour associated with twin jets in close proximity. *Expl Therm. Fluid Sci.* **69**, 127–140.